Progress In Electromagnetics Research C, Vol. 40, 53–68, 2013

ON THE DESIGN OF ULTRA WIDE BAND RECTANGULAR SLOT ANTENNA EXCITED BY A FLARED MICROSTRIP FEED LINE

Rajas Khokle[1], Raj Kumar[2], and Raghupatruni Venkatsiva Ram Krishna[3, *]

[1]LEOC-21, Department of Applied Physics, DIAT, Deemed University, Girinagar, Pune 411025, India

[2]ARDE, Pashan, Pune 411021, India

[3]Department of Electronics Engineering, DIAT, Deemed University, Girinagar, Pune 411025, India

Abstract—A rectangular slot antenna for UWB applications is proposed in this paper. The slot is designed in stepped configuration and is excited by an L-shaped microstrip line flared at the end. The measured impedance bandwidth (-10 dB) from 3 GHz to 27 GHz is achieved. The radiation patterns are bidirectional in the E plane and omnidirectional in the H plane with the measured peak gain around 5 dBi throughout the band. The experimental results are in good agreement with the simulated results. A detail parametric study is done for the flare angle and the flare width to axis ratio and their effect on the impedance bandwidth and the reflection coefficient is described.

1. INTRODUCTION

The requirement of compact and efficient antennas capable of operating in the entire ultra wideband frequency range defined by the Federal Communications Commission (FCC) (from 3.1 GHz to 10.6 GHz) is seen to be rapidly increasing. This is due to an explosive increase in the number of small portable devices operating for different wireless applications [1]. Among the various antenna configurations possible, the microstrip fed slot is particularly attractive due to the features like simpler design, low profile planar structure, wider bandwidth, bidirectional/omni-directional radiation patterns and increased degree

Received 6 April 2013, Accepted 10 May 2013, Scheduled 21 May 2013

* Corresponding author: Raghupatruni Venkatsiva Ram Krishna (rk_nedes@yahoo.co.in).

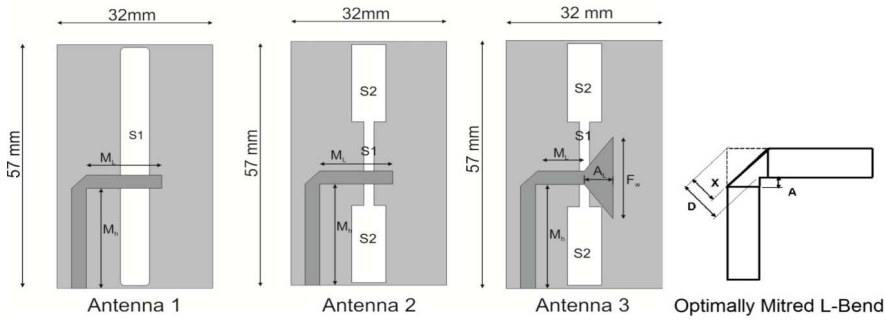

Figure 1. Evolution of antenna.

of freedom for applying impedance matching techniques to get a wider bandwidth.

A simple rectangular slot fed using a microstrip feed has been studied theoretically and experimentally in the past. However, most of the designs were meant for narrow band operation and the studies focussed on the first resonance of the slot. Some of the rectangular slot antennas designed for wider bandwidth are listed in references [2–6]. In [2], a dual band operation is achieved by the combination of a narrow slot and slot loop. In [3], an L-shaped strip is introduced in a slot to achieve the dual wideband characteristics. A wide impedance bandwidth of 2.4 GHz using two fictitious shorts at the slot end was reported by Nadar et al. in [4]. A CPW fed slot antenna for wide band applications was proposed in [5]. It covered the frequency range from 2.1 GHz to 3.6 GHz by dividing the slot into sections of different widths on either side of the CPW feed. Another CPW fed T-shaped slot was reported in [6], in which the impedance bandwidth achieved was 5.7 GHz.

In this paper, a rectangular slot antenna with stepped sections and fed by an optimally mitred L-shaped microstrip feed is proposed. The feed is terminated by a flared microstrip stub. This helps in reducing the overall size of the antenna and ensures a better impedance matching over a wider bandwidth. The −10 dB simulated impedance bandwidth starts from 3 GHz with the lower end primarily being decided by the dimensions of the slot as well as the flared section of the feed. A description of the evolution process of the antenna is given in Section 2 followed by discussion on the measured and simulated results in the subsequent sections. A parametric study showing the effects of various design parameters is also included. The antenna is expected to be useful for portable devices operating in the UWB spectrum.

2. ANTENNA DESIGN AND EVOLUTION

The antenna design is an evolutionary process which can be divided into three distinct phases as shown in Figure 1. All the antennas are designed on easily available FR4 substrate with $\varepsilon_r = 4.4$, thickness 1.58 mm and $\tan\delta = 0.02$. The overall dimensions of the antenna are 57 mm × 32 mm. The slot is etched on the ground plane and excited by an L-shaped microstrip line from the other side of the substrate. In order to match the impedance of the microstrip line to the standard 50 Ω SMA connector, the width of the microstrip line is calculated to be 3 mm by using Equations (1) and (2) originally given in [7].

$$\frac{W}{h} = \frac{8e^A}{e^{2A}-2} \tag{1}$$

$$A = \frac{z_0}{60}\frac{\sqrt{\epsilon_r+1}}{2} + \frac{(\epsilon_r-1)}{\epsilon_r+1}\left(0.23+\frac{0.11}{\epsilon_r}\right) \tag{2}$$

The L bend introduces a discontinuity in the microstrip line which can be represented by a shunt capacitance. In order to reduce its effect, the L bend is mitred optimally at 45^0 using the empirical expressions (Equations (3), (4), & (5)) given by Douville and James [8].

$$D = W\sqrt{2} \tag{3}$$

$$X = D\left(0.52+0.65\exp\left(-13.5\frac{W}{h}\right)\right) \tag{4}$$

$$A = \left(X-\frac{D}{2}\right)\sqrt{2} \tag{5}$$

A slot shorted at both the ends has minimum voltage at the terminating ends. Consequently, the maximum voltage will be at the centre. Hence a slot offers maximum impedance at the centre [9, 10] and it becomes difficult to match such high impedance to a standard 50 Ω microstrip line. To overcome this, the microstrip line feeds the slot at an offset from centre as suggested by Yoshimura [11]. The dimensions corresponding to the labels shown in Figure 1 are indicated in Table 1.

Next, the development of the slot is discussed. Initially, to study the wideband characteristics of the slot, a graph of the input impedance (Z_{11}) as a function of p/λ for a simple slot antenna with an offset feed is plotted as shown in Figure 2, where p is the perimeter of the slot and λ is the effective wavelength in the substrate. From this graph, it can be seen that there is less variation in the real part of the impedance in the region where $p/\lambda = 2$. Also the imaginary part of Z_{11} is nearly zero in this region. From the simulation studies, it is also observed that there

Table 1. Optimized dimensions of antennas.

Antenna 1	Label	S_1		M_L		M_H	--		--	
	Parameter	L_1	W_1	L_{ML}	W_{ML}	23.75	--	--	--	--
	Value (mm)	55.5	6	15.5	3		--	--	--	--
Antenna 2	Label	S_1		S_2		M_L	M_H		--	
	Parameter	L_1	W_1	L_2	W_2	14.6	23.75		--	--
	Value (mm)	19.5	2.1	18	7				--	--
Antenna 3	Label	S_1		S_2		M_L	M_H		Flare	
	Parameter	L_1	W_1	L_2	W_2	9.58	23.75		A_L	F_w
	Value (mm)	19.5	2.1	18	7				5.9	18.66

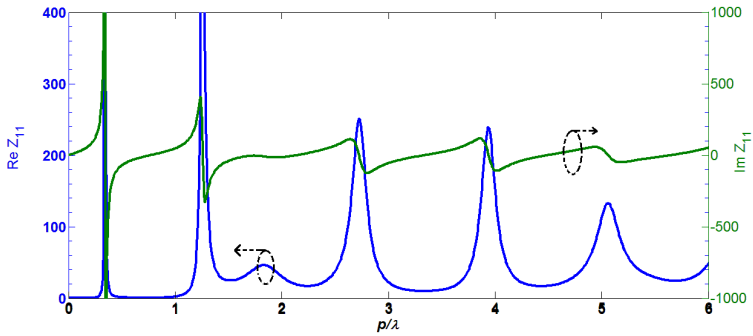

Figure 2. Real and imaginary part of impedance (Z_{11}) of Antenna-1 as a function of p/λ.

is reduction in impedance of the structure when the ground beyond the slot is decreased. Considering this, a single moderately wide slot having dimensions 55.5 mm × 6 mm is etched on the 57 mm × 32 mm ground plane, as shown in Figure 1 (Antenna 1). This slot is fed by the microstrip line offset from the centre and terminated in an

open circuited stub which is used for tuning the resonant frequency of the slot. With the given slot perimeter and tuning stub length, the resonance is obtained at 3.4 GHz with bandwidth from 3.1 GHz to 3.9 GHz.

To obtain multiple resonances, a stepped impedance structure is utilized as shown in Antenna 2. The theoretical analysis of such a stepped impedance slot resonator was presented in [12] using the transmission line equations. It was shown in [12] that the resonant frequency for such a slot configuration depends not only on the lengths of the sections but also on the impedance ratio of the two sections. Also, as suggested in [13], the slot-line region near the feed-line should have lesser width in order to achieve a better transfer of electromagnetic energy from the microstrip line to the slot while the width of the remaining slot-line should be more in order to achieve enlarged radiation aperture. The resonant frequencies for such a configuration can be further altered by loading the microstrip feed line with open circuit microstrip stub. The effect of varying the stub length on the reflection coefficient is shown in Figure 3.

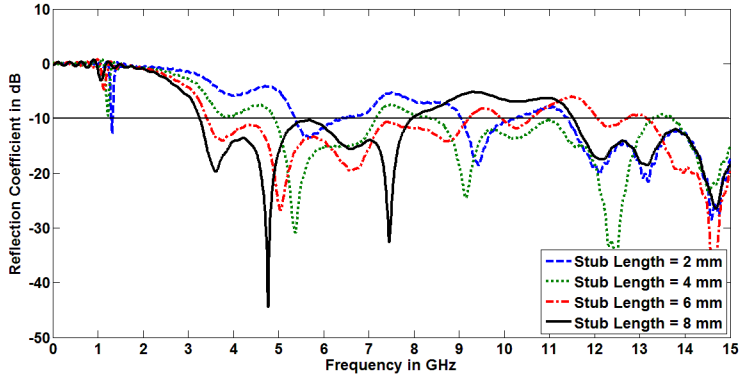

Figure 3. Effect of microstrip stub length on the reflection coefficient of Antenna 2.

It is observed that as the stub length increases, the lowest resonant frequency shifts to a still lower value. However, the higher frequencies also shift to the lower side. So it is not possible to achieve good impedance matching over the entire FCC UWB bandwidth just by varying the stub length.

It can be noted that the stub acts as an open circuit termination for the microstrip line which increases the capacitance of the structure and can be used to tune the frequency over which the slot resonates. Alternatively, the capacitance of the microstrip line can be increased

by increasing the width of the microstrip line. However, changing the width also changes the impedance of the line. To obtain a smoother change in impedance as well as capacitance, the microstrip line is flared from the centre of the slot to obtain the geometry of Antenna 3. The angle of flare and the ratio of flare width to the stub length (axis) are the critical parameters for obtaining good impedance matching over the entire bandwidth. A comparison of the simulated S_{11} for the three antennas is given in Figure 4. It can be observed that an extra resonance at 6.8 GHz is obtained for Antenna 2 as compared with Antenna 1 while Antenna 3 gives a good impedance matching over the entire bandwidth.

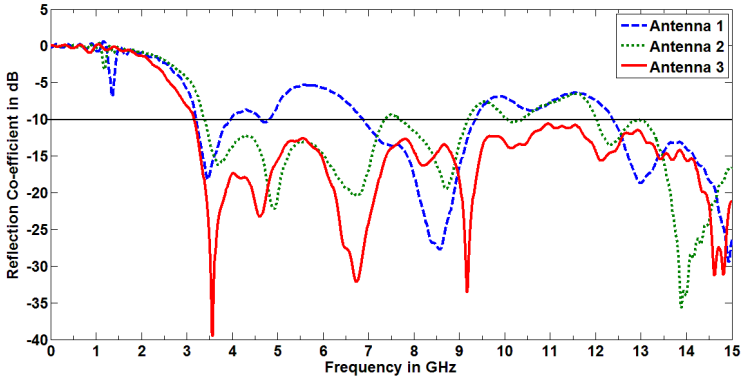

Figure 4. Comparison of the simulated S_{11} curves of the three antennas.

3. RESULTS AND DISCUSSION

3.1. Reflection Coefficient

The Antenna 3 is fabricated and tested for the reflection coefficient and radiation characteristics. A photograph of the fabricated antenna is given in Figure 5. The antenna is simulated in CST microwave studio using transient solver as well as in Ansoft HFSS using frequency domain solver. The comparison of simulated and experimental results is shown in Figure 6. The -10 dB bandwidth starts from 3 GHz and extends to 27 GHz. Here it can be seen that the experimental result closely follows the simulated result especially at lower frequencies. A slight difference in the simulated and experimental results may be due to uncertainties in the relative permittivity of the substrate used as

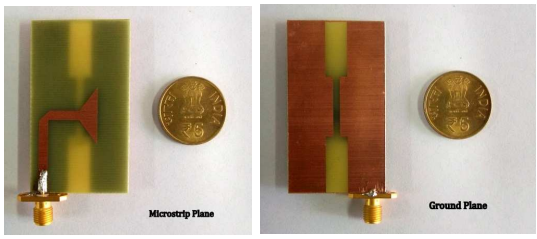

Figure 5. Photograph of the fabricated slot antenna.

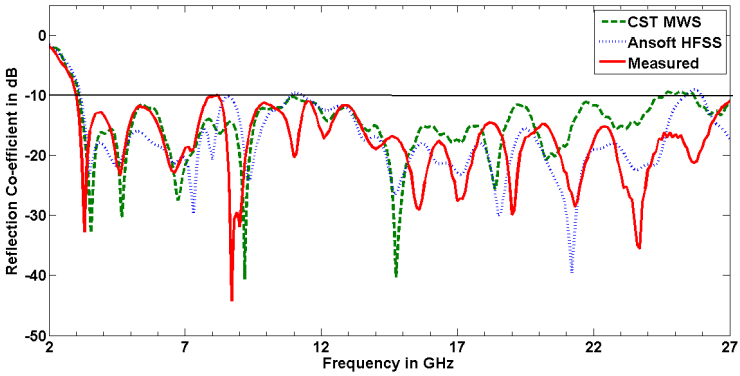

Figure 6. Comparison of simulated and measured reflection coefficient of the proposed antenna.

well as due to the expansion of the Teflon inside the connector due to soldering which is unavoidable.

3.2. Radiation Patterns

The radiation patterns of the proposed antenna are measured by an antenna measurement system placed in an anechoic chamber. The system comprises of a reference horn antenna (Schwarzbeck BBHA 9120C) working from 3 to 18 GHz and placed at a distance of 1 m from a turn-table on which the proposed antenna is mounted. The orientation of the antenna in the XY plane is such that the slot length is along the Y direction which makes the XZ plane as the E plane and YZ plane as the H plane. The measured results are plotted along with the HFSS and CST simulated patterns in Figure 7. From the figures, a good agreement can be seen between the measured and simulated radiation patterns. It is further observed that at lower frequencies, the E-Plane patterns resemble the figure of eight indicating bidirectional

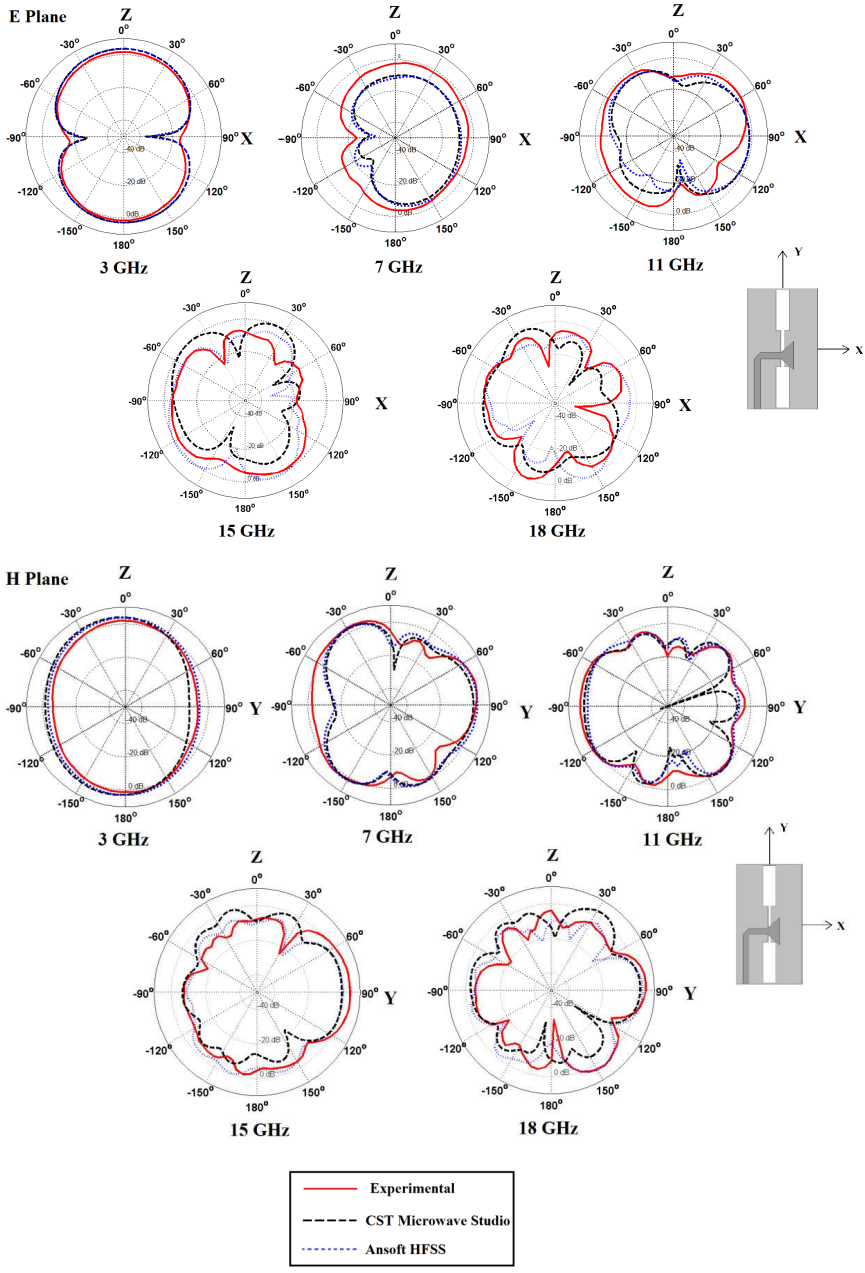

Figure 7. Polar plots of radiation pattern in the two principle planes; XZ (E-Plane) and YZ (H-Plane) for 3 GHz, 7GHz, 11 GHz 15 GHz and 18 GHz.

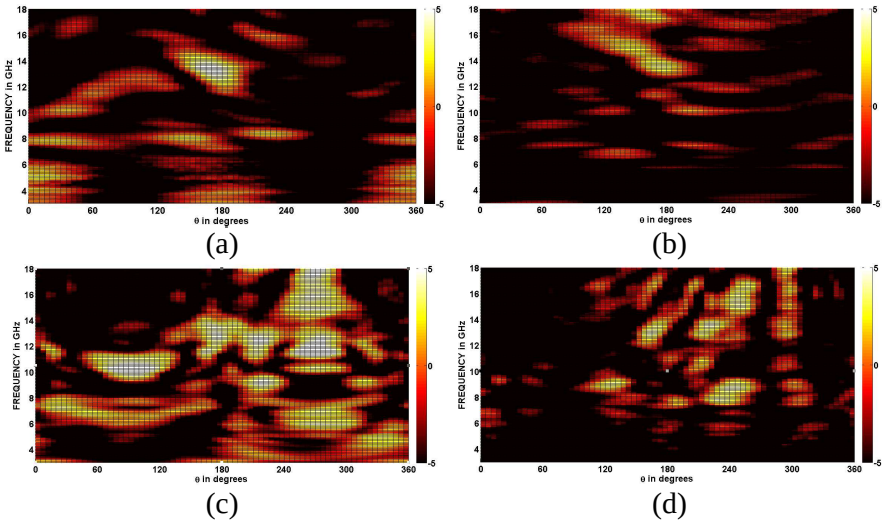

Figure 8. Radiation characteristics in E and H plane as a function of frequency. (a) E plane co polarization. (b) E plane cross polarization. (c) H plane co polarization. (d) H plane cross polarization.

characteristics while the H-Plane patterns are nearly omni-directional and resemble a circle in shape. At higher frequencies, the patterns become distorted due to increased cross-polarization and the presence of higher order modes. A 2D plot of the co and cross-polarization as a function of the angle θ and the frequency in both the E-Plane and H-Plane is shown in Figure 8 which further confirms the increase in cross polarization levels at higher frequencies (upper region).

3.3. Peak Gain and Radiation Efficiency

The measured peak gain is taken to be the maximum gain value from either the E plane or H plane pattern (whichever is large). The measured peak gain of the proposed antenna as a function of the frequency is shown in Figure 9 alongside the HFSS and CST simulated results. The simulated radiation efficiency is shown in Figure 10. From the gain plot, a good matching between the simulated and measured values is observed over most of the frequencies. An initial low value in the measured gain (up to 3 GHz) is primarily due to the characteristics of the reference horn antenna whose operating region is specified to be from 3 GHz to 18 GHz. The average gain of the proposed antenna is 4.7 dB over the complete band. The radiation efficiency decreases with increase in frequency. This decrease is due to the increased losses in

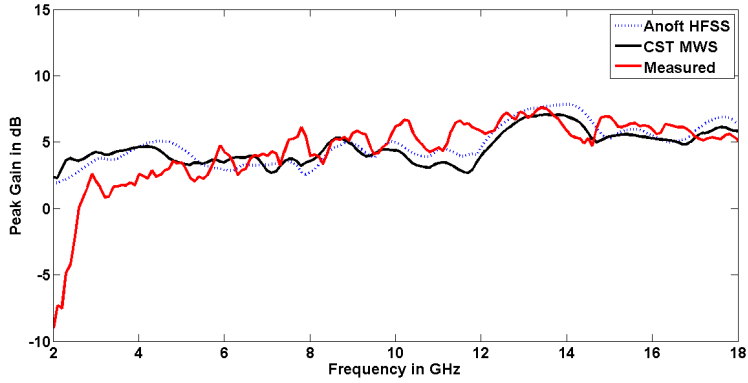

Figure 9. Measured and simulated peak gain of the proposed antenna.

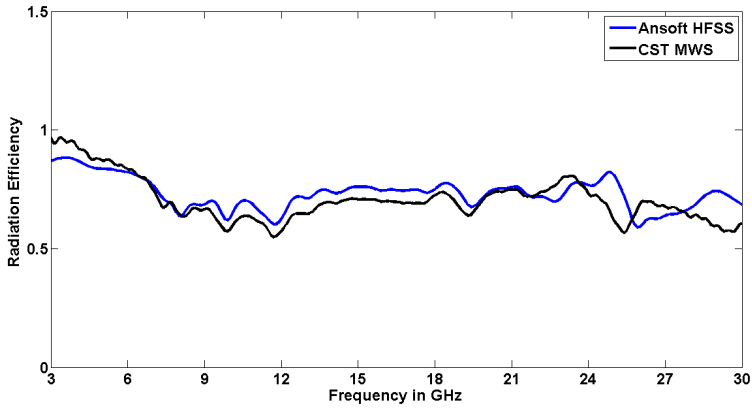

Figure 10. Simulated radiation efficiency of the proposed antenna.

the substrate at higher frequencies. Also as the frequency increases, the structure becomes electrically large and the smaller wavelength is unable to excite the complete structure efficiently.

4. PARAMETRIC STUDIES

The L-shaped microstrip feed exciting the stepped slot is terminated on a flared stub whose axial length (A_L) and flare width (F_w) control the wideband impedance matching. The effect of varying the axial length and the flare angle on the S_{11} characteristic is shown in Figure 11 and Figure 12 respectively. While varying the length, the flare angle was kept constant and vice versa. It is seen that a smaller length gives a

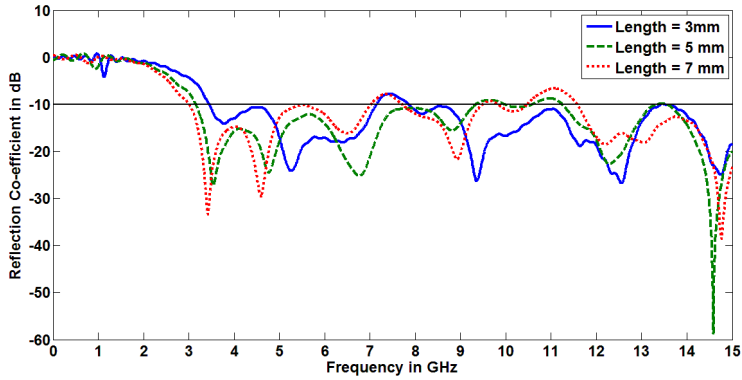

Figure 11. Effect of the axial length (A_L) on the S_{11} characteristic.

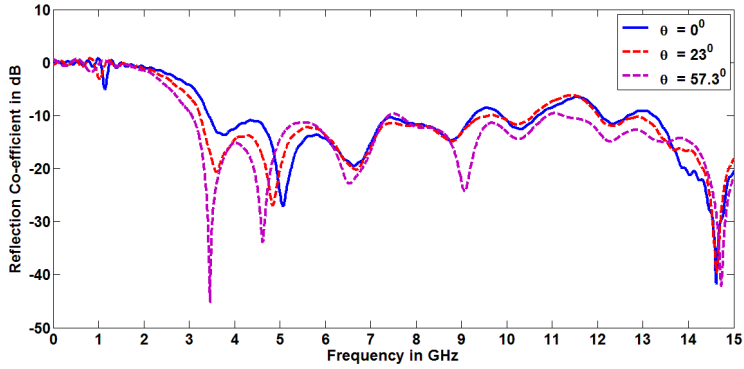

Figure 12. Effect of varying the flare angle on S_{11} with constant feed length.

better impedance matching at higher frequencies while a larger length improves the impedance matching at lower frequencies. Also, increase in the length decreases the lower edge frequency. From Figure 12, it can be observed that an increase in the flare angle improves the impedance matching over the entire bandwidth especially at lower frequencies. However, due to the geometrical constraints, the flare angle cannot be increased beyond a limit and an optimal value for both the length and the flare angle has to be found.

To further study the effect of flaring, a graph of the ratio F_w/A_L versus the first resonant frequency for various axis lengths is plotted in Figure 13. It is found that for a fixed length, as the ratio F_w/A_L goes

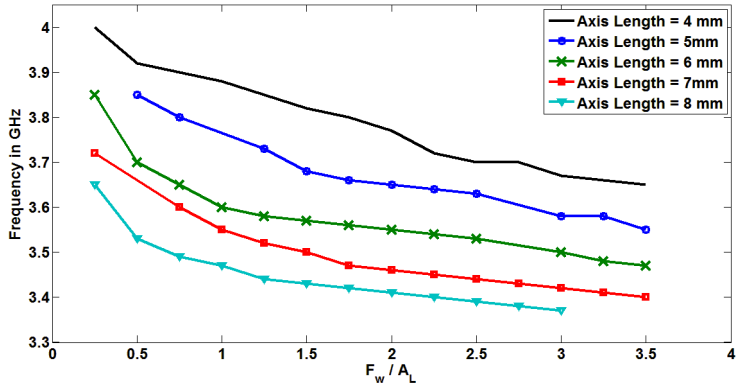

Figure 13. Ratio (F_w/A_L) vs. frequency for different axis lengths.

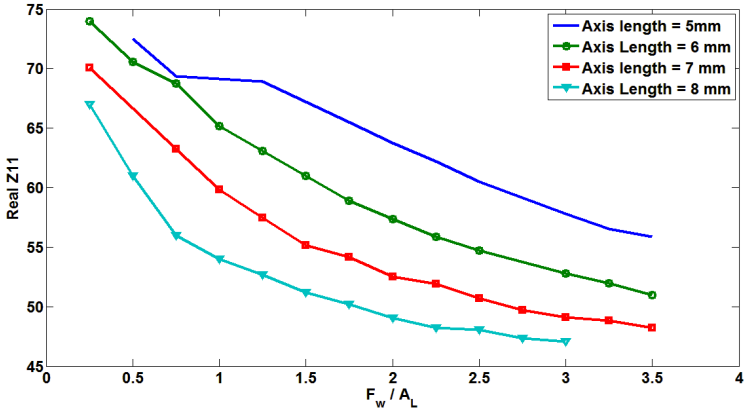

Figure 14. Ratio F_w/A_L vs. real part of Z_{11} at first resonance for various axis lengths.

on increasing the resonant frequency goes on decreasing. Thus we can achieve lower resonant frequency without increasing the overall size of the antenna.

The effect of the ratio F_w/A_L on the real part of the input impedance at the first resonant frequency is shown in Figure 14. Here, a set of curves are plotted for different values of the axis length.

As the ratio F_w/A_L increases, the impedance at the first resonance decreases as seen from Figure 14. As a consequence there exists an optimum value for which the impedance of the structure will match

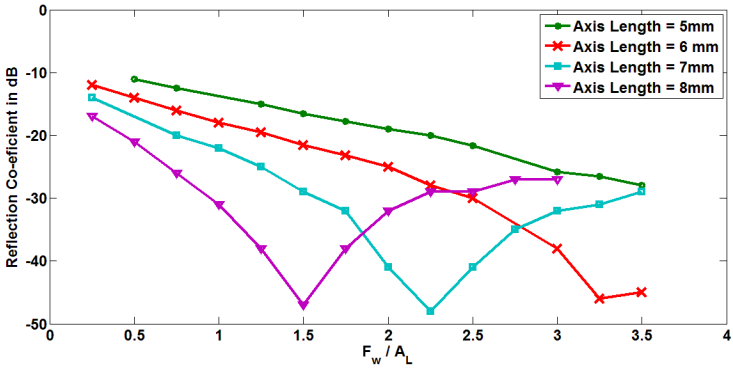

Figure 15. Ratio (F_w/A_L) vs. reflection coefficient for various axis lengths.

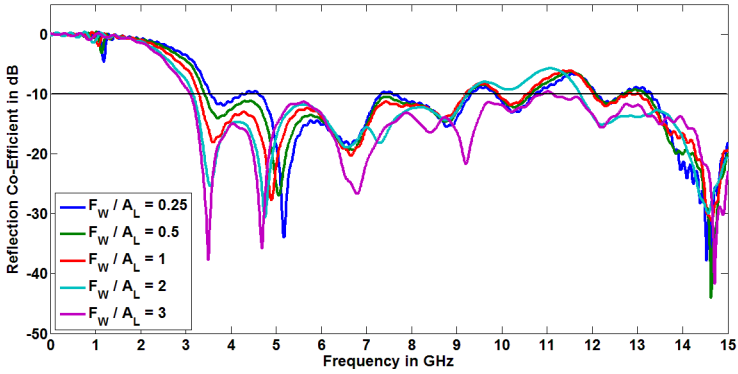

Figure 16. Effect of ratio (F_w/A_L) on reflection coefficient at axis length = 6 mm.

with the 50 Ω generator. A further decrease in impedance will cause impedance mismatch and so reflection coefficient will increase. This can be validated from Figure 15 in which the reflection coefficient at the first resonance versus the ratio F_w/A_L is plotted for different axis lengths. The graph for $A_L = 8$ mm distinctly shows the behaviour described above. The impedance matching in this case is obtained for $F_w/A_L = 1.5$.

Again, referring to Figure 14, it is seen that the decrease in impedance is not linear and shows a saturation behaviour. In order to get a quantitative idea, curve fitting is done and generalized Equation (6) is formulated. Here Z_i is the input impedance at the

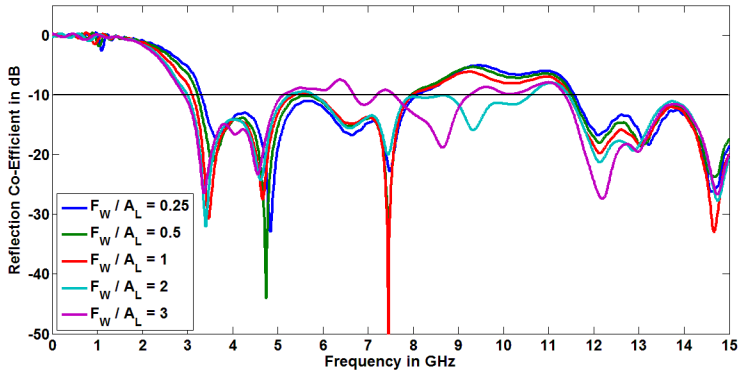

Figure 17. Effect of ratio (F_w/A_L) on reflection coefficient at axis length = 8 mm.

first resonance and expressed as a function of F_w/A_L while Z_0 and x are variables depending on the axis length A_L as given by Equations (7) and (8) respectively.

$$\mathrm{Re}(Z_i) = Z_0(F_w/A_L)^x \tag{6}$$

$$\text{where } Z_0 = -4.694A_L + 91.75 \tag{7}$$

$$x = -0.1915\exp(-0.03086A_L) + 0.9378\exp(-0.6875A_L) \tag{8}$$

From these equations, it can be observed that as the axis length is increased, the coefficients 'Z_0' and 'x' go on decreasing. This signifies that the fall in impedance is rapid for higher axis lengths but the characteristics reach to saturation behaviour earlier, i.e., for lesser values of F_w/A_L. To check the validity of this analysis for higher resonances the S_{11} curves for different ratios for two different axis lengths 6 mm and 8 mm are as plotted respectively in Figures 16 and 17. It can be seen that, while the better impedance matching for entire bandwidth is obtained at $F_w/A_L = 3$ for axis length = 6 mm, similar response is obtained at $F_w/A_L = 2$ for axis length = 8 mm. However, it can be noted that the impedance for 8 mm is less than impedance for 6 mm curve (Figure 14), so there is more impedance mismatch with axis length = 8 mm which can also be observed by comparing the curves of $F_w/A_L = 3$ of Figure 16 and $F_w/A_L = 2$ of Figure 17. In light of these parametric studies, further optimization in the design is done and the optimum value with respect to bandwidth and reasonably good reflection coefficient over entire bandwidth is found to be at axis length = 5.9 mm and $F_w/A_L = 3.16$.

5. CONCLUSION

A simple design of a rectangular slot antenna with a microstrip L-shaped flared feed is proposed in this paper. The slot and feed line are suitably modified to get the best impedance characteristics. The impedance bandwidth is from 3 GHz to 27 GHz which is well beyond the UWB range defined by the FCC. The antenna has a reasonably constant peak gain around 5 dBi and is expected to be useful for present and future applications in wireless communication devices operating in the UWB region.

ACKNOWLEDGMENT

The first author is a graduate student at Defence Institute of Advanced Technology (Deemed University), Pune, India and acknowledges the financial support and facilities extended for carrying out the research work.

REFERENCES

1. Yang, L. and G. B. Giannakis, "Ultra-wideband communications: An idea whose time has come," *IEEE Signal Processing Magazine*, Vol. 21, No. 6, 26–54, Nov. 2004.
2. Chulvanich, C., J. Nakasuwan, N. Songthanapitak, N. Anantrasirichai, and T. Wakabayashi, "Design narrow slot antenna for dual frequency," *PIERS Online*, Vol. 3, No. 7, 1024–1028, 2007.
3. Khunead, G., J. Nakasuwan, N. Songthanapitak, and N. Anantrasirichai, "Investigate rectangular slot antenna with L-shaped strip," *PIERS Online*, Vol. 3, No. 7, 1076–1079, 2007.
4. Behdad, N., K. Sarabandi, Fellow IEEE, "A multiresonant single-element wideband slot antenna," *IEEE Antennas and Wireless Propagation Letters*, Vol. 3, No. 1, 5–8, 2004.
5. Nithisopa, K., J. Nakasuwan, N. Songthanapitak, N. Anantrasirichai, and T. Wakabayashi, "Design CPW fed slot antenna for wideband applications," *PIERS Online*, Vol. 3, No. 7, 1124–1127, 2007.
6. Jiao, J.-J., G. Zhao, F.-S. Zhang, H.-W. Yuan, and Y.-C. Jiao, "A broadband CPW-fed T-shape slot antenna," *Progress In Electromagnetic Research*, Vol. 76, 237–242, 2007.

7. Pozar, D. M., *Microwave Engineering*, 4th Edition, John Wiley & Sons Inc., 2011.
8. Douville, R. J. P. and D. S. James, "Experimental study of symmetric microstrip bends and their compensation," *IEEE Transactions on Microwave Theory and Techniques*, Vol. 26, 175–181, 1978.
9. Gupta, K. C., R. Garg , I. J. Bahl, and P. Bhartia, *Microstrip Lines and Slotlines*, 2nd Edition, Artech House Publications, 1996.
10. Kim, J. P. and W. S. Park, "Network modeling of an inclined and off-center microstrip-fed slot antenna," *IEEE Transactions on Antennas and Propagation*, Vol. 46, No. 8, 1182–1188, 1998.
11. Yoshimura, Y., "A microstripline slot antenna (short papers)," *IEEE Transactions on Microwave Theory and Techniques*, Vol. 20, No. 11, 760–762, 1972.
12. Tu, W.-H. and K. Chang, "Miniaturized CPW-fed slot antenna using stepped impedance resonator," *2005 IEEE Antennas and Propagation Society International Symposium*, Vol. 4A, 351–354, 2005.
13. Huang, X. D., C. H. Cheng, and L. Zhu, "An ultrawideband (UWB) slotline antenna under multiple-mode resonance," *IEEE Transactions on Antennas and Propagation*, Vol. 60, No. 1, 385–389, 2012.